IET Generation, Transmission & Distribution

Research Article

IET Journals
The Institution of Engineering and Technology

ISSN 1751-8644
doi：0000000000
www.ietdl.org

Application of generative adversarial network-based optimization approach to energy storage allocation in power systems

Cheng-Yi Lin[1], *Shyh-Jier Huang*[1]*

[1] *Department of Electrical Engineering, National Cheng Kung University, Tainan, Taiwan*
* *E-mail: clhuang@mail.ncku.edu.tw*

Abstract: This study applies the generative adversarial network-based optimization approach to site selection and capacity determination of energy storage device in a power grid. Through the combination of modified long short-term memory and generative adversarial networks, the proposed method enhances the learning capability for the decision support of energy storage allocation. This method excels at the utilization of modified long short-term memory to ensure a better data-generation and data-discrimination in a generative adversarial network, enabling the achievement of effective data learning and deduction. To validate the feasibility of the proposed approach, a practical system as well as an example system are both examined under different scenarios, where the placement cost, peak load, and voltage deviation are all concerned. Test results gained from this study are beneficial for energy storage industry applications. In this study, a novel approach is proposed for site selection and capacity determination of energy storage devices in power grids by applying a generative adversarial network-based optimization method. The proposed approach combines modified long short-term memory and generative adversarial networks to enhance the learning capability for decision support of energy storage allocation. Specifically, the modified long short-term memory improves the data-generation and data-discrimination in the generative adversarial network, leading to effective data learning and deduction. To demonstrate the feasibility of our proposed approach, a practical system as well as an example system are tested under different scenarios, where the placement cost, peak load, and voltage deviation are all taken into considerations. Test results indicate the feasibility of the method, providing valuable insights for the energy storage industry.

1 Introduction

The rapid advancement of battery manufacturing technology has made energy storage devices a critical solution for addressing the issue of energy shortages. Energy storage devices offer flexible charging and discharging mechanisms, allowing them to charge during off-peak hours and supply power to the grid during peak times, which significantly reduces grid congestion [1]-[2]. Moreover, energy storage devices can be integrated with monitoring and communication devices to regulate their real and reactive power output. This integration helps to mitigate voltage and frequency variations caused by load changes and improve the quality of supplied power [3]-[4].

Previous literature has addressed the decision-making methods for determining the capacity and charge/discharge scheduling of single energy storage devices [5]-[7]. Energy storage is known for enhancing the continuity of power supply during intermittent generation due to weather changes [8]-[10]. Additionally, energy storage devices can regulate power over a brief period since their charge/discharge reaction is faster than that of conventional thermal power generating units, providing higher flexibility to the dispatching operation. With the emergence of microgrids, energy storage devices are increasingly being installed to adapt to load changes and assist in handling islanding operations once the grid is disconnected from mains power [11]-[13]. Although these studies have been effective in grid operation, they have been limited in overall performance assessment of energy storage placement. Therefore, intelligent approaches such as genetic algorithms and particle swarm optimization have been employed for solution search [14]-[15]. However, their computation procedures may not consider capacity, leading to the inadvertent utilization of energy storage and ineffective planning. More attention is needed to address this issue for a better allocation of energy storage equipment.

This paper integrates the photovoltaic system with an energy storage device to complement the insufficient supply of the solar system while minimizing the impact on the grid, particularly during night peak loading periods. The study aims to simultaneously determine the site and capacity of the energy storage device, including reactive power regulation [16]-[20]. To facilitate the computation, this study proposes a generative adversarial network (GAN) with modifications, embedding long short-term memory (LSTM) for memory gating mechanisms in both data generator and discriminator within the network. This gating control simplifies memory inference and accelerates computation convergence [21]-[26]. Furthermore, the generative adversarial network is powerful in creating datasets for testing, and model simulation accuracy is improved via learning from massive datasets.

This article begins by investigating power flow simulation to understand system features, focusing on scenarios that involve the integration of photovoltaics and wind power with the grid. Mathematical models of multi-objective functions are formulated while considering planning costs, peak load, and voltage deviation. Next, a generative adversarial network-based optimization approach is applied to establish a trained network with inference capability for the site selection and capacity determination of energy storage devices in a power grid. This method has three notable features:

1) It systematically determines the optimal allocation of energy storage devices by considering site and capacity,

where total operation cost, peak load, and voltage deviation are all included.

2) This study proposes a solution approach to reinforce the training model, enabling effective inference of energy storage planning under different grid-connection conditions.

3) The scheme of proposed algorithm is well-organized and expandable. This method can be also cooperated with other commercial software for utility planning applications. The proposed algorithm scheme is well-organized and expandable. Additionally, it can be easily integrated with other commercial software for utility planning applications.

The organization of this paper is as follows: Section 2 formulates the problem of energy storage device planning, Section 3 presents the proposed method, Section 4 describes the numerical tests, and Section 5 draws conclusions.

2 Energy storage planning

Fig. 1 illustrates the block diagrams of energy storage devices. The primary objective of integrating energy storage systems with the grid is to regulate power flow rapidly and address dispatch issues, ultimately improving the reliability of power supply. The use of energy storage devices also helps alleviate the pressure of load demand during peak hours [27]-[30]. The charging and discharging states of an energy storage device are expressed as follows:

$$E_i^t = E_i^{t-1} + \beta P_i^t \Delta t \tag{1}$$

where E_i is the charging status of the i^{th} energy storage device at time t, E_i^{t-1} is the initial charging of the i^{th} energy storage device, P_i^t represents the charging power of the i^{th} energy storage device at time t, Δt is the duration of charging, and β is the charging efficiency. Conversely, the discharging status can be expressed as follows:

$$E_i^t = E_i^{t-1} - \frac{1}{\beta} P_i^t \Delta t \tag{2}$$

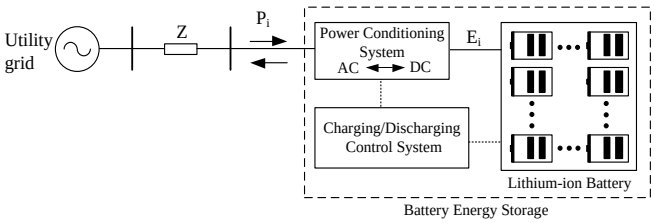

Fig. 1. Block diagrams of energy storage devices

To ensure that the energy storage device operates within the allowable limits, the following constraints are provided:

$$K_{\min} E_{r,i} \le E_i^t \le K_{\max} E_{r,i} \tag{3}$$

$$0 \le N_{ess} \le N_{bus} \tag{4}$$

$$V_{\min} \le V_p \le V_{\max} \tag{5}$$

Next, Eq. (5) is used to express the voltage limits, where V_p is the voltage of the p^{th} bus, and V_{min}, V_{max} are the upper and lower limit of the bus voltage, respectively. Based on the above operating limits, the study next includes the planning cost, peak load, and voltage deviation as the objectives for the formulation of multi-objective functions. First, the planning cost of energy storage device consists of installation cost and line loss. The installation cost is related with the number of devices and their individual capacity, which is expressed below:

As expressed in Eq. (3), $E_{r,i}$ represents the rated capacity of the i^{th} energy storage device, while K_{min} and K_{max} are constants used to ensure a reasonable output of energy storage devices. Additionally, Eq. (4) specifies that the number of installed energy storage devices must not exceed the total number of system buses. Here, N_{ess} represents the number of energy storage devices, and N_{bus} represents the number of buses in the system. Eq. (5) is used to express the voltage limits, where V_p is the voltage of the p^{th} bus, and V_{min} and V_{max} represent the lower and upper limits of the bus voltage, respectively. Based on these operating limits, the study then includes planning cost, peak load, and voltage deviation as objectives in the formulation of multi-objective functions. The planning cost of the energy storage device comprises the installation cost and line loss. The installation cost is related to the number of devices and their individual capacity, as expressed below:

$$C_e = c_e \sum_{n=1}^{Ness} E_{r,n} \tag{6}$$

where C_e is the installation cost of energy storage device, c_e is the cost per unit storage capacity, N_{ess} is the number of devices installed, and $E_{r,n}$ is the capacity of the n^{th} energy storage device. In addition to installation cost, the line loss is concerned here, which can be computed using the following equation:

$$P_{loss} = \sum_{i=1}^{Ng} P_G^i + \sum_{j=1}^{Nc} P_{DG}^j - \sum_{k=1}^{N_k} P_L^k \pm \sum_{l=1}^{Ne} P_{es}^l \tag{7}$$

where P_{loss} is the amount of line loss, P_G^i is the generated power, P_{DG}^j is the generation of distributed generators, P_L^k is the load power, $\pm P_{es}^l$ is the inflow or outflow of real power of the energy storage device, N_g is the number of generating units, N_c is the number of distributed generators, N_e is the number of energy storage devices, and N_k is the number of load buses. The cost of line loss is then calculated as follows:

$$C_{loss} = e_{loss} \sum_{d=1}^{M_y} M_d P_{loss} \tag{8}$$

$$C_{total} = C_e + C_{loss} \tag{9}$$

Eq. (9) can be normalized as follows:

$$f_1 = \frac{C_{total} - C_{\min}}{C_{\max} - C_{\min}} \tag{10}$$

where C_{min} and C_{max} is the minimum and the maximum planning cost. Subsequently, the second objective function considered is the determination of the peak load, which is calculated as follows

$$P_{pk} = \max_{t=1,\ldots,24} (P_{L,t}) \tag{11}$$

where P_{pk} is the maximum load of the system, and $P_{L,t}$ is the load at the t hour. This objective function can be also preprocessed as below

$$f_2 = \frac{P_{pk} - P_{pk,\min}}{P_{pk,max} - P_{pk,\min}} \tag{12}$$

where $P_{pk,max}$ and $P_{pk,min}$ is the maximum and the minimum value of the peak load. Next, the third objective function is voltage deviation, which is calculated below

$$V_D = \max_{n=1,\ldots,N_{bus}} \left(\frac{|V_{rated} - V_n|}{|V_{rated}|}\right) \times 100\ \% \tag{13}$$

where V_D is the maximum rate of voltage deviation, V_{rated} is

the rated bus voltage, and V_n is the n-th bus voltage. This objective function is normalized below

$$f_3 = \frac{V_D - V_{D,\min}}{V_{D,\max} - V_{D,\min}} \tag{14}$$

where $V_{D,max}$ and $V_{D,min}$ is the maximum and the minimum percentage of voltage deviation rate. The multi-objective function is formulated by combining f_1, f_2 and f_3 equations (10), (12), and (14), respectively. The resulting function can be summarized as follows:

$$f_{obj} = \min\left(w_1 f_1 + w_2 f_2 + w_3 f_3\right) \tag{15}$$

The individual weight of f_1, f_2 and f_3 are denoted by w_1, w_2 and w_3, respectively, and can be adjusted according to planning needs. With these weights, the model formulation of energy storage allocation is complete.

3 Generative adversarial network-based optimization approach

This study employs a modified approach based on generative adversarial networks (GANs) to analyze and determine the optimal site and capacity for energy storage devices. By incorporating the long short-term memory neural network (LSTM), the study introduces a modified version called the modified long short-term memory neural network (MLSTM). This MLSTM is integrated with the generator and discriminator of the GANs, resulting in an enhanced learning process. The following sections provide a detailed explanation of this integrated approach.

The long short-term memory (LSTM) neural network is a recurrent neural network known for its utilization of three gates to regulate data transmission. However, when confronted with larger training datasets, the multiplication of the gating matrix within LSTM can lead to an increase in computational burden, subsequently impacting convergence performance. Hence, this study proposes an enhanced gating mechanism as a modification to the network. This modification eliminates the need for temporary output addition from the previous layer, while still maintaining satisfactory learning performance in subsequent propagation layers. In essence, the study adjusts the weight of the temporary output Y_{t-1} in the previous layer to zero and investigates the propagation neuron of the gating mechanism.

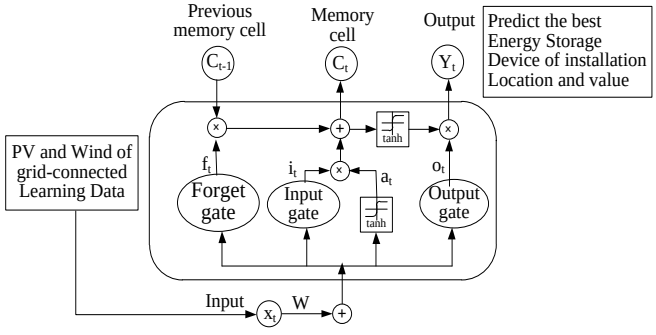

Fig. 2 Modified LSTM model

Fig. 2 illustrates the modified long short-term memory neural network, displaying the output equations for the input gate, filter gate, and output gate as listed below:

$$i_t = \tanh\left(W_i x_t + b_i\right) \tag{16}$$

$$f_t = \tanh\left(W_f x_t + b_f\right) \tag{17}$$

$$o_t = \tanh\left(W_o x_t + b_o\right) \tag{18}$$

where x_t is the input neuron value at time t, which corresponds to the capacity of the current power transmission system when renewable energy is integrated. The data points are multiplied by the output weights and augmented with an offset (b_i, b_f, and b_o) of 0.1. These multiplication results are subsequently filtered and passed through the nonlinear activation function (*tanh*) to derive the modified gate output. It is important to note that cross-validation is also employed in this process to ensure effective data learning.

Following the validation of MLSTM, the study proceeds to investigate the application of generative adversarial networks as the solution approach for energy storage placement. Fig. 3 illustrates the employed GAN for this study, wherein the data generator generates or fabricates data to feed the network. The discriminator, on the other hand, distinguishes differences and extracts relevant information. Through the learning process, the generated data and real data become increasingly similar, significantly reducing the required size of the training dataset. The underlying principle of this network lies in the use of maximum likelihood estimation. It involves establishing a probability distribution function $P_d(x)$ based on the real input data, where x represents data points within the dataset. Consequently, a probability distribution function $P_g(z)$ is initially constructed based on the generator's content. By adjusting $P_g(z)$ to satisfy the condition of $P_d = P_g$, the optimal solution can be achieved.

Based on the principle of equilibrium mentioned above, this study utilizes the generator to produce samples that reflect the intermittent power generation of photovoltaics and wind turbines. Subsequently, the discriminator is employed to extract useful data for decision support regarding the location and capacity of energy storage devices. To enhance computational performance, the MLSTM is adopted to replace traditional neural networks within the generator and discriminator of the original generative adversarial network. Essentially, the objective of Fig. 3 is to optimize memory cell and gating mechanisms to guide the generated data towards real data, enabling the trained neural network to extract crucial information and exhibit superior inference capability. In this modified generative adversarial network, the generator's input is obtained through a random variable z, which is then filtered by the MLSTM network to approximate the distribution of real data with $G(z)$. These data are subsequently fed into the discriminator alongside real data, training the network to capture representative relationships and serve as decision support for the problem concerned.

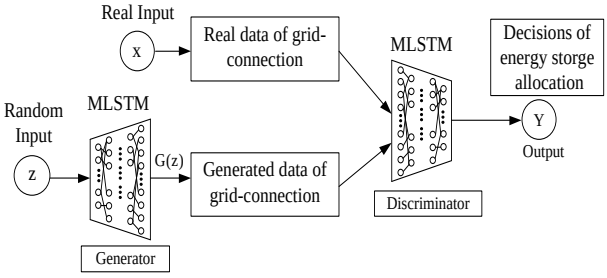

Fig. 3 Block diagram of proposed method including the modified generative adversarial network

4 Computation procedure

Fig. 4 illustrates the flowchart of the proposed method, with the main computation blocks outlined as follows:

Step 1) Initialization of parameters

The computation initializes with the data collected from the utility, including energy storage capacity, available locations, neural network parameters, and operating limits.

Step 2) Construction of database

In this step, load flow computation is conducted to determine the operating status of the power system, incorporating the presence of renewable energy sources at different buses. Subsequently, the location and capacity of energy storage devices are simulated, providing information such as line loss, bus voltage magnitude, and planning cost. These data are then collected to form a database for training the discriminator model.

Step 3) Construction of data generator model

During this step, a normally distributed power generation profile for renewable energy is randomly generated. This generated profile is utilized for training the MLSTM network, as shown in Fig. 2. The nonlinear activation function, *tanh*, is employed for the network neurons with an offset of 0.1. The output value of $G(z)$ is normalized within the range of [-1, 1]. Once the data regarding grid-connected power generation is captured, the corresponding location and capacity of the energy storage device can be inferred and prepared for further verification.

Step 4) Confirmation of discriminator model

In this study, the discriminator is constructed using the MLSTM architecture. It receives both real load flow data and data generated from the network for training purposes. During the training process, the learning rate is initially set at 0.05 and gradually decreased. The cross-validation technique is also implemented to ensure the effectiveness of the trained discriminator.

Step 5) Process termination

During the training process, once the maximum number of training epochs is reached and the convergence condition is met, the relevant parameters are stored, and the training is terminated. Subsequently, utilizing the data of grid-connected generation as input to this modified generative adversarial network, the network determines and presents output information, including the location and capacity of energy storage devices.

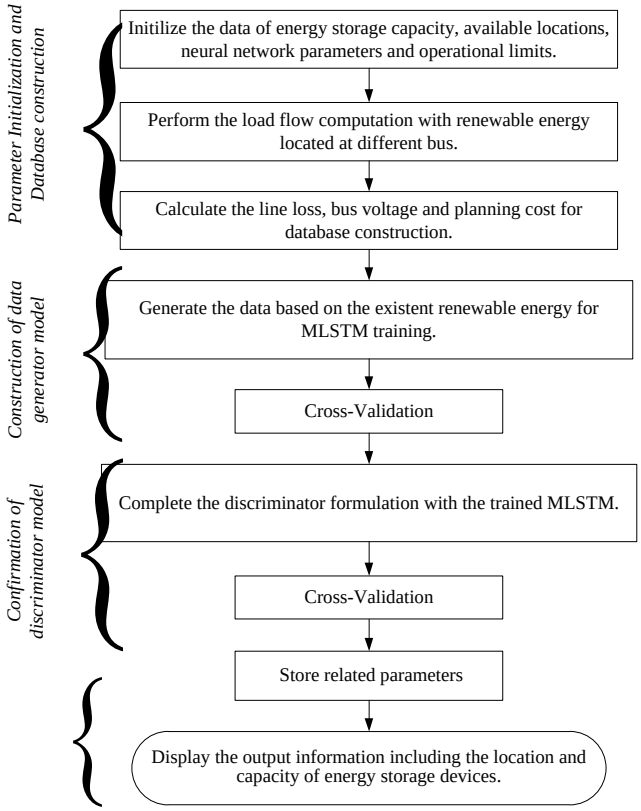

***Fig. 3** Flowchart of proposed method*

5 Numerical simulations

The proposed approach has been evaluated on a subset of the Taiwan power system [31] and the IEEE 30-bus system [32]. In Fig. 4, the 14-bus system located in southern Taiwan is depicted with the swing bus at bus #1, and photovoltaic and wind power generation at bus #13 and #14, respectively. The energy storage device's charging and discharging mechanism helps regulate the grid's supply and demand, enabling better control of voltage changes at each bus in the system. Lithium-ion batteries are selected as the primary components of the energy storage device due to their high energy density. In this study, the energy capacity is set at 300 MWh, the power capacity at 30 MW, and the charging/discharging efficiency at 90%. To account for the durability and usage of lithium-ion batteries, their lifetime is set at 10 years [33]. The installation cost is assumed to be \$80/MWh, and the line loss cost is \$2.1/kWh, based on a published report [34]. Safety measures include setting the upper and lower voltage limits for each bus in the system at 1.0 p.u. and 0.9 p.u., respectively. The proposed method is implemented in the Python programming language. We investigate four scenarios: Test 1, 2, and 4 on the practical 14-bus system, and Test 3 on the IEEE 30-bus system.

5.1 Test 1

By considering hourly load changes and intermittent power after the integration of photovoltaic generation with wind power, both methods of the original generative adversarial network and the proposed approach are applied to determine the location and capacity of energy storage devices. Factors such as placement cost, peak load, and voltage deviation are considered during this process. In this test scenario, the real power load is 426 MW, and the reactive power load is 94 Mvar. Fig. 5 illustrates the photovoltaic and wind power

generation for this test system, where photovoltaic generation with a capacity of 5 MW is installed at bus #13, and wind power generation with a capacity of 30 MW is installed at bus #14.

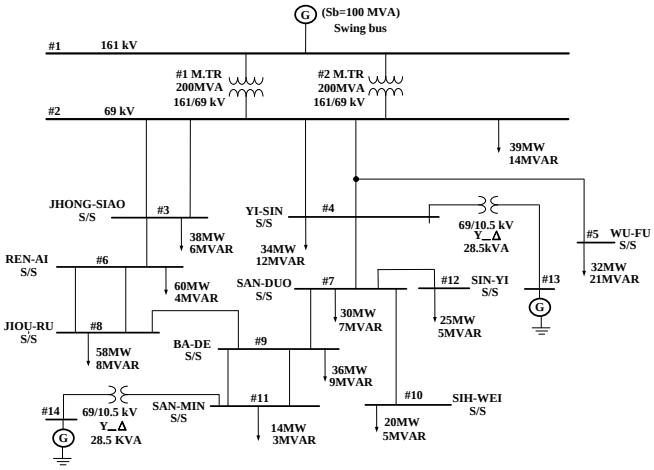

***Fig. 4** Test system*

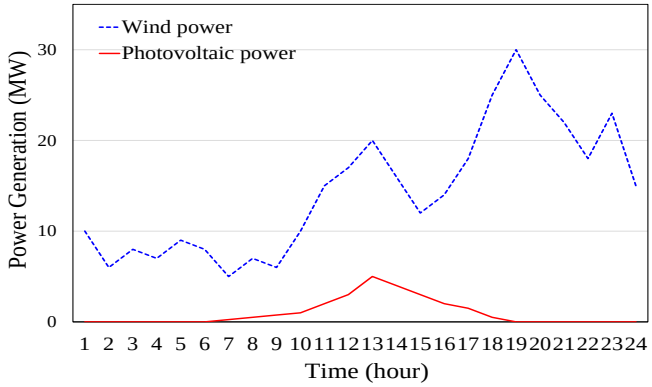

***Fig. 5** Photovoltaic and wind power generation.*

The computation begins by employing the Newton-Raphson method to simulate the power flow, incorporating energy storage devices with capacities of 10, 15, 20, 25, and 30 MW connected to their corresponding buses. The real power status and line loss data are obtained to establish the dataset. Note that bus #1, #13, and #14 are excluded from this analysis as they serve as either swing buses or reserved locations for renewable energy placement. Simulation results for energy storage allocation are presented in Table 1. Two methods are evaluated in this simulation: Method 1 employs the original generative adversarial networks (GAN), while Method 2 utilizes the proposed approach. Three groups of energy storage devices are allocated in this test. Fig. 6 illustrates the charging and discharging schedules for these devices, with charging occurring from 1 to 6 am and from 10 pm to 12 am, and discharging taking place from 7 am to 7 pm. Fig. 7 compares the load demand with and without the proposed method, demonstrating effective peak burden alleviation facilitated by the energy storage devices. Additionally, Fig. 8 shows the voltage deviation rate calculated with and without the proposed approach. The proposed method significantly reduces the deviation rate, effectively maintaining bus voltages within predetermined values.

Table 1 Simulation results of grid-connected energy storage devices for Test 1

Energy storage device No.	Method 1 (Original GAN)		Method 2 (Proposed Method)	
	Location (Bus)	Capacity (MWh)	Location (Bus)	Capacity (MWh)
1	4	190	3	195
2	8	250	8	245
3	11	250	12	245

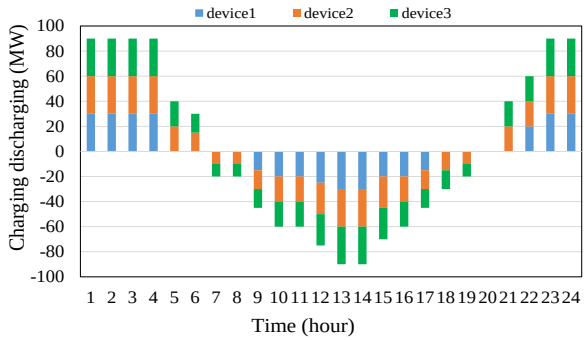

***Fig. 6** Charging and discharging schedule of energy storage devices*

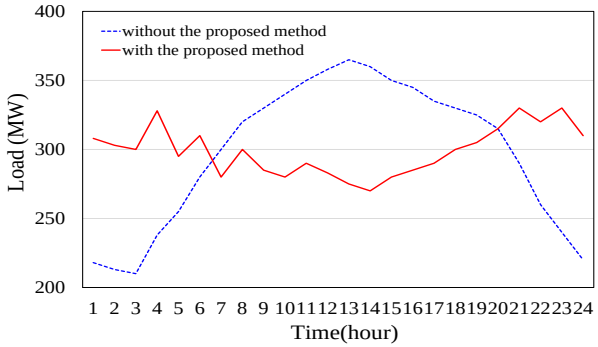

***Fig. 7** Load demand with and without the proposed method*

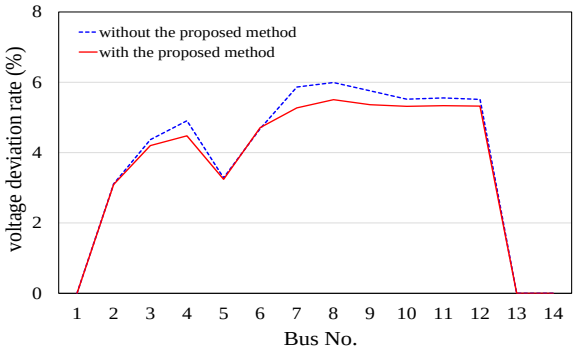

***Fig. 8** Voltage deviation rate of each bus for Test 1*

5.2 Test 2

This test focuses on determining the optimal location and capacity of an energy storage device within a power grid that features a larger-scale integration of photovoltaic generation. Its purpose is to evaluate the feasibility of the proposed method in addressing the night peak demand observed in Taiwan. As the amount of photovoltaic power generation declines after sunset, energy storage devices must activate rapidly to meet the grid's requirements. The simulation conducted in this study involves a photovoltaic generation system with a capacity of 60 MW installed at bus #13 and #14, supplying power from 7 am to 5 pm [35]. The objectives encompass total operation cost, peak load

management, and voltage deviation mitigation.

Table 2 presents the computation results obtained using the proposed method, allowing for a comparison with another existing approach. The table provides details on the installation location and capacity of four groups of energy storage devices. Fig. 9 illustrates the charging and discharging schedule of these energy storage devices, while Fig. 10 showcases the load variation when the energy storage devices are employed. These figures demonstrate that the proposed method effectively addresses the issue of the night peak demand. Fig. 11 displays the voltage deviation rate at each bus, highlighting that both methods are effective in maintaining a satisfactory voltage deviation rate.

Table 2 Simulation results of grid-connected energy storage devices for Test 2

Energy storage device No.	Method 1 (Original GAN)		Method 2 (Proposed Method)	
	Location (Bus)	Capacity (MWh)	Location (Bus)	Capacity (MWh)
1	3	80	3	80
2	7	165	5	160
3	8	270	9	260
4	10	160	12	160

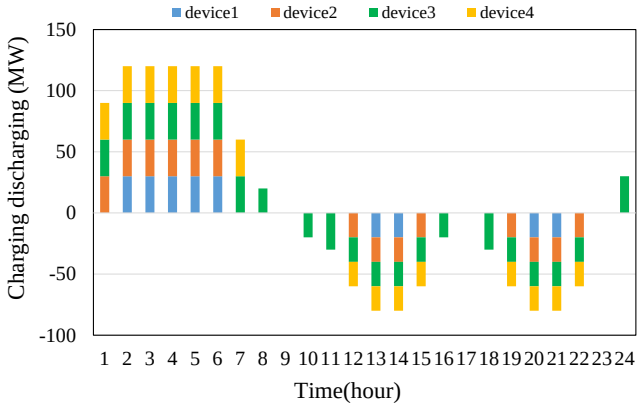

***Fig. 9** Charging and discharging schedule of energy storage devices*

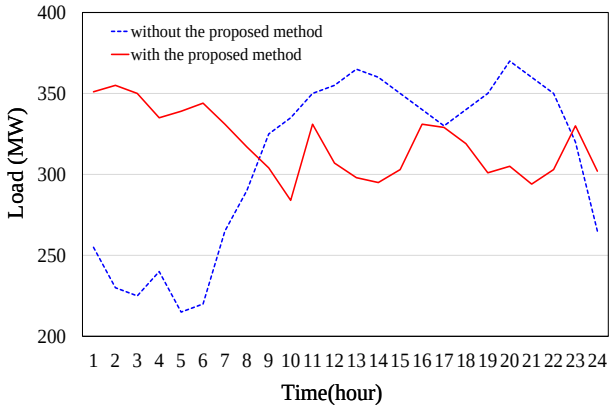

***Fig. 10** Load demand with assistance of energy storage devices.*

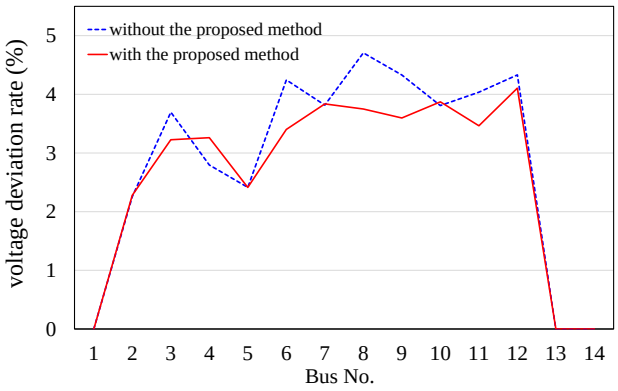

***Fig. 11** Voltage deviation rate of each bus for Test 2*

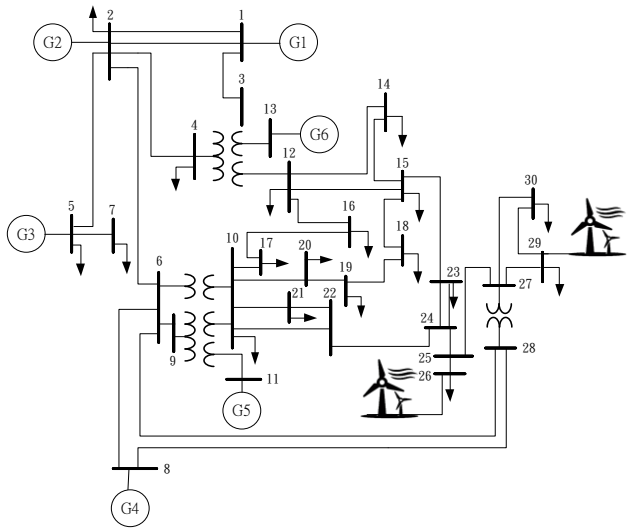

***Fig. 12** IEEE 30-bus system*

5.3 Test 3

This case study focuses on simulating the provision of reactive power by an energy storage device through a power conversion system. Fig. 12 depicts an IEEE 30-bus system, where wind power is integrated at Bus #26 and #29. The objective is to stabilize the bus voltage variations resulting from the intermittent nature of wind power generation through the regulation of reactive power from the energy storage devices. The total real power in this case is 402 MW, while the total reactive power is 188 Mvar. The wind farm's generators have a power capacity of 30 MW, representing a high proportion of renewable energy generation. The study specifically investigates an energy storage device with a capacity of 60 MVA and a reactive power output of 36 Mvar, aimed at regulating the system voltage [36].

As this case study prioritizes the average load rather than the peak load, the weights assigned to ω_1, ω_2 and ω_3, representing the placement cost, peak load, and voltage deviation respectively, are set as 1, 0, and 1 in the objective function formulation. The computation results for energy storage allocation concerning reactive power are presented in Table 3. The table specifies the location and capacity of the energy storage devices for different wind generation outputs ranging from 10 MW to 30 MW. Two sets of energy storage devices are considered, with placement options at Bus #18 and #24, or Bus #18 and #25. Fig. 13 illustrates the voltage deviation rate with and without the proposed method. Both methods exhibit a maximum voltage deviation of approximately 12%.

Fig.14 presents the simulation results for voltage

variation under various levels of wind power penetration. In each of the five wind power penetration cases, the placement of energy storage devices assists in keeping the voltage of each bus close to 0.9 p.u. This outcome confirms the method's effectiveness in enhancing voltage stability.

Table 3 Computation results of energy storage allocation consideration the provision of reactive power.

No.	Wind (MW)	Energy Storage	
		Location (Bus)	Reactive power (Mvar)
1	10	18	-36
		24	-36
2	15	18	-35
		25	-35
3	20	18	-34
		24	-34
4	25	18	-25
		24	-25
5	30	18	-24
		24	-24

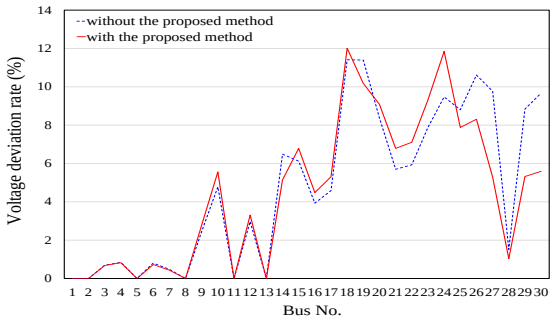

Fig. 13 *Voltage deviation rate of each bus for Test 3.*

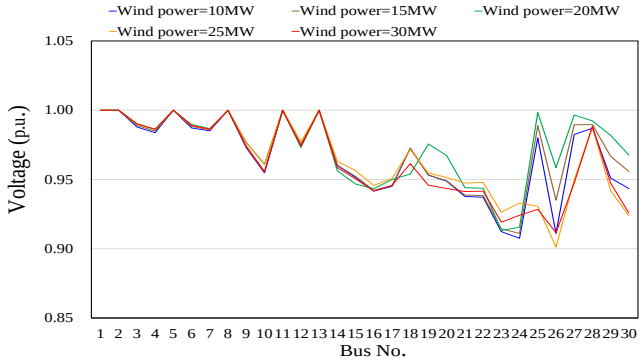

Fig. 14 *Voltage variation under different penetrations of wind power generations.*

5.4 Test 4

This case study investigates the optimal placement of energy storage devices in the presence of wind power integration within the grid. The motivation behind this study arises from the impact of the strong northeast monsoon in Taiwan during winter, which leads to significant fluctuations in power generation throughout the day, thereby affecting the stability of power supply. Fig. 15 provides a schematic diagram illustrating the integration of wind power with energy storage devices. To ensure the grid's normal operation, the existing approach relies on charging the batteries during off-peak hours and discharging them during peak hours. However, the substantial difference between the maximum and minimum wind power generation exceeding 220 MW may result in considerable voltage fluctuations, potentially compromising the quality of busbar voltage. To mitigate this issue, a power conversion system (PCS) is employed to convert wind power into DC for storage and subsequently convert it back to AC for grid integration. This PCS solution prompts the simulation test conducted here to evaluate the optimal placement of energy storage devices under this scenario.

In this simulation test, the conversion efficiency of the PCS (AC to DC) is set at 90%, and the weights assigned to the total placement cost, peak load, and voltage deviation are individually set at 0, 1, and 1 in the formulation of the objective function. Based on the data collected from the average wind power generation in Taiwan, the highest and lowest wind power generation values are recorded as 280 MW and 60 MW, respectively, as depicted in Fig.16.

This test commences with a power flow calculation to identify suitable locations for wind power allocation. Bus #11, #12, #13, and #14 are identified as appropriate locations. Using the proposed method, Bus #11 and #12 are selected for energy storage device allocation. The next step involves determining the capacity of each energy storage device for different periods of wind power generation. Table 4 presents the computation results for energy storage allocation during the first, fourth, eighth, thirteenth, seventeenth, and twenty-first hour.

Based on the information in Table 4, Figure 17 illustrates the charging periods from 1 am to 8 am, 4 pm to 5 pm, and 10 pm to 12 am, as well as the discharging periods from 9 am to 3 pm and 6 pm to 9 pm. The maximum charging capacity is 254 MW, while the maximum discharging capacity is 190 MW. These charging and discharging schedules align with the load variation trend of the considered transmission system, effectively balancing the power grid's supply and demand. Furthermore, Fig. 18 depicts the voltage at each busbar of the power grid at the 13th hour (1 pm), reflecting that none of the bus voltages fall below 0.9 p.u. This test demonstrates the method's effectiveness in providing stability support to the system.

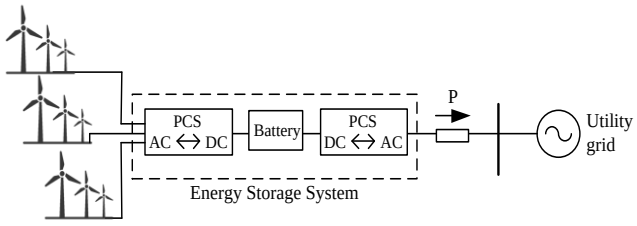

Fig. 15 *Schematic diagram of wind power integrated with energy storage device*

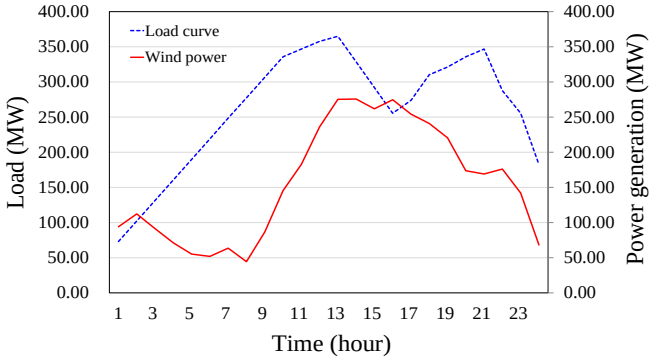

Fig. 16 *Load curve and wind power generation.*

Table 4 Computation results of energy storage allocation for each period of wind power generation

Time	Wind (MW)	Energy Storage Location (Bus)	Energy Storage Capacity (MWh)
1	94.03	11	42.02
		12	52.01
4	71.17	11	23.0
		12	48.17
8	44.36	11	26.74
		12	17.62
13	275.31	11	165.31
		12	110.0
17	254.22	11	142.0
		12	112.22
21	169.07	11	75.07
		12	94.0

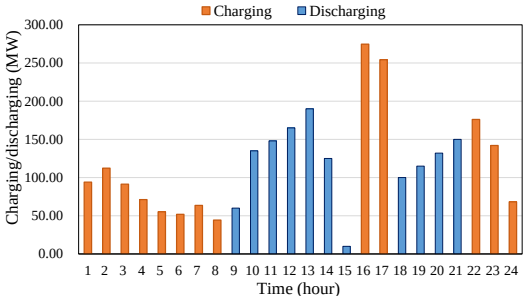

***Fig. 17** Charging and discharging schedule of energy storage device*

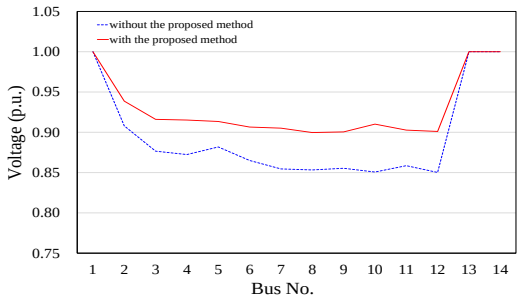

***Fig. 18** Voltage fluctuation value of each bus at the 13th hour for Test 4.*

6 Conclusions

This study proposes a modified generative adversarial network-based optimization approach to improve decision-making support for energy storage device placement. The proposed method combines modified long short-term memory with generative adversarial networks to intelligently allocate energy storage. Practical feasibility tests have been conducted on a real power grid using utility data. The results demonstrate that the proposed approach effectively reduces costs and improves voltage profiles through optimized energy storage placement. This advancement facilitates planning automation and paves the way towards a greener power network.

7 Acknowledgments

The authors are greatly indebted to Taiwan Power Company for providing their valuable operating experiences.

8 References

[1] J. Dong, F. Gao, X. Guan, Q. Zhai, and J. Wu, "Storage Sizing with Peak-Shaving Policy for Wind Farm Based on Cyclic Markov Chain Model," *IEEE Transactions on Sustainable Energy*, Vo1.8, No.3, pp.978-989, July 2017.

[2] S. U. Agamah, and L. Ekonomou, "Peak Demand Shaving and Load-Levelling Using a Combination of Bin Packing and Subset Sum Algorithms for Electrical Energy Storage System Scheduling," *IET Science, Measurement & Technology*, Vol. 10, No. 5, pp. 477-484, August 2016.

[3] A. DiGiorgio, F. Liberati, A. Lanna, A. Pietrabissa, and F.D. Priscoli, "Model Predictive Control of Energy Storage Systems for Power Tracking and Shaving in Distribution Grids," *IEEE Transactions on Sustainable Energy*, Vol. 8, No. 2, pp.496-504, April 2017.

[4] E. Ghahremani, and I. Kamwa, "Optimal Allocation of STATCOM with Energy Storage to Improve Power System Performance," *IEEE Transmission and Distribution* Conference, Chicago, USA, April 2014.

[5] N. Jayasekara, M. A. S. Masoum, and P. J Wolfs, "Optimal Operation of Distributed Energy Storage Systems to Improve Distribution Network Load and Generation Hosting Capability," *IEEE Transactions on Sustainable Energy*, Vol. 7, No. 1, pp. 250-261, January 2016.

[6] A. Nagarajan and R. Ayyanar, "Design and Strategy for the Deployment of Energy Storage Systems in a Distribution Feeder with Penetration of Renewable Resources," *IEEE Transaction on Sustainable Energy*, Vol. 6, No. 3, pp.1085-1092, July 2015.

[7] X. Ke, N. Lu, and C. Jin, "Control and Size Energy Storage Systems for Managing Energy Imbalance of Variable Generation Resources," *IEEE Transactions on Sustainable Energy*, Vol. 6, No. 1, pp. 70-78, January 2015.

[8] N. Li and K. W. Hedman, "Economic Assessment of Energy Storage in Systems with High Levels of Renewable Resource," *IEEE Transactions on Sustainable Energy*, Vol. 6, No. 3, pp. 1103-1111, July 2015.

[9] P. Zou, Q. Chen, Q. Xia, G. He, and C. Kang, "Evaluating the Contribution of Energy Storages to Support Large-Scale Renewable Generation in Joint Energy and Ancillary Service Markets," *IEEE Transactions on Sustainable Energy*, Vol. 7, No. 2, pp. 808-818, April 2016.

[10] K. Rahbar, C. C. Chai, and R. Zhang, "Energy Cooperation Optimization in Microgrids with Renewable Energy Integration," *IEEE Transactions on Smart Grid*, Vol. 9, No. 2, pp.1482-1493, March 2018.

[11] B. Liu, F. Zhuo, Y. Zhu, and H. Yi, "Systems Operation and Energy Management of a Renewable Energy-Based DC Micro-Grid," *IET Renewable Power Generation*, Vol. 8, No. 1, pp. 45-57, January 2014.

[12] S. Singh, M. Singh, and S. C. Kaushik, "Optimal Power Scheduling of Renewable Energy Systems in Microgrids Using Distributed Energy Storage System," *IET Renewable Power Generation*, Vol. 10, No. 9, pp. 1328-1339, October 2016.

[13] Y. Han, X. Xie, H. Deng, and W. Ma, "Central Energy Management Method for Photovoltaic DC Micro-Grid System Based on Power Tracking Control," *IET Renewable Power Generation*, Vol. 11, No. 8, pp. 11388-1147, June 2017.

[14] D. B. Liu, L. J. Shi, Q. Xu, W. J. Du, and H. F. Wang, "Selection of Installing Locations of Flywheel Energy Storage System in Multimachine Power Systems by Model Analysis," *International Conference on Sustainable Power Generation and Supply*, Nanjing, China, pp. 1-4, April 2009.

[15] X. Huang, G. Zhang, and L. Xiao. "Optimal Location of SMES for Improving Power System Voltage Stability," *IEEE Transactions on Applied Superconductivity*, Vol. 20, No. 3, pp. 1316-1319, June 2010.

[16] D. Lew and N. Miller, "Reaching New Solar Heights: Integrating High Penetrations of PV into the Power System," *IET Renewable Power Generation*, Vol. 11, No. 1, pp. 20-26, April 2017.

[17] F. Marra, G Yang, C. Traeholt, J. Ostergaard, and E. Larsen, "A Decentralized Storage Strategy for Residential Feeders with Photovoltaics," *IEEE Transactions on Smart Grid*, Vo1. 5, No. 2, pp. 974-981, March 2014.

[18] A. Hassan and Y. Dvorkin, "Energy Storage Siting and Sizing in Coordinated Distribution and Transmission Systems," *IEEE Transactions on Sustainable Energy*, Vol. 9, No. 4, pp. 1692-1701, October 2018.

[19] A. D. Giorgio, F. Liberati, A. Lanna, A. Pietrabissa, and F.D. Priscoli, "Model Predictive Control of Energy Storage Systems for Power Tracking and Shaving in Distribution Grid," *IEEE Transactions on Sustainable Energy*, Vol. 8, No. 2, pp. 496-504, April 2017.

[20] X. Ke, N. Lu, and C. Jin, "Control and Size Energy Storage Systems for Managing Energy Imbalance of Variable Generation Resources," *IEEE Transactions on Sustainable Energy*, Vol. 6, No. 1, pp. 70-78, January 2015.

[21] J. Zheng, C. Xu, Z. Zhang, and X. Li, "Electric Load Forecasting in Smart Grids Using Long-Short-Term-Memory based Recurrent Neural Network," *Annual Conference on Information Sciences and Systems*, Baltimore, USA, pp. 1-6, March 2017.

[22] Y. Lu and F. M. Salem, "Simplified Gating in Long Short-term Memory(LSTM) Recurrent Neural Networks," *International Midwest Symposium on Circuits and Systems*, Boston, USA, pp. 1601-1604, August 2017.
[23] F. Zhang, C. Hu, Q. Yin, W. Li, H.C. Lin, and W. Hong, "Multi-Aspect-Aware Bidirectional LSTM Networks for Synthetic Aperture Radar Target Recognition," *IEEE Access,* Vol. 5, pp. 26880-26891, November 2017.
[24] A. Creswell, T. White, V. Dumoulin, K. Arulkumaran, B. Sengupta and A. Bharath, "Generative Adversarial Network- An Overview," *IEEE Signal Processing Magazine,* Vol. 35, No. 1, pp. 53-65, January 2018.
[25] Y. Chen, Y. Wang, D. Kirschen, and B. Zhang, "Model-Free Renewable Scenario Generation Using Generative Adversarial Networks," *IEEE Transactions on Power Systems*, Vol. 33, No. 3, pp. 3265-3275, May 2018.
[26] Y. Xiang and C. Bao, "Speech Enhancement Via Generative Adversarial LSTM Networks," *International Workshop on Acoustic Signal Enhancement*, Tokyo Japan, pp. 46-50, September 2018.
[27] J. Xiao, Z. Zhang, L. Bai, and H. Liang, "Determination of the Optimal Installation Site and Capacity of Battery Energy Storage System in Distribution Network Integrated with Distributed Generation," *IET Generation, Transmission & Distribution*, Vol. 10, No. 3, pp. 601-607, March 2016.
[28] H. Y. Lin, "Application of Enhanced Grasshopper Algorithm to Decision Support for Placement of and Capacity Selection of Energy-Storage Devices," *Master Thesis*, National Cheng Kung University, Taiwan, 2019.
[29] G. Carpinelli, G. Celli, S. Mocci, F. Mottola, F. Pilo, and D. Proto, "Optimal Integration of Distributed Energy Storage Devices in Smart Grids," *IEEE Transactions on Smart Grid*, Vol. 4, No. 2, pp. 985-995, June 2013.
[30] Q. Zhang, J. He, and D. Zhang, "Coordinated Control of Energy Storage Devices and Photovoltaic Inverters for Voltage Regulation Based on Multi-Agent System," *International Conference on Energy Internet and Energy System Integration*, Beijing, China, pp. 1-6, November 2017.
[31] Taiwan Power Company, "System Line and Load Parameters of Tainan Primary Substation Area," July 2017.
[32] I. Totonchi, H. Akash, A. Akash, and A. Faza, "Sensitivity Analysis for the IEEE 30 Bus System Using Load-flow Studies," *International Conference on Electric Power and Energy Conversion System*, Istanbul, Turkey, pp. 1-6, October 2013.
[33] R. Fernander-Blanco, Y. Dvorkin, B. Xu, Y. Wang, and D. S. Kirschen, "Optimal Energy Storage Siting and Sizing: A WECC Case Study," *IEEE Transactions on Sustainable Energy*, Vol. 8, No. 2, pp. 733-743, April 2017.
[34] International Renewable Energy Agency, "Electricity Storage and Renewables: Costs and Markets to 2030," October 2017.
[35] H. O. R. Howlader, M. Furukakoi, H. Matayoshi, and T. Senjyu, "Duck Curve Problem Solving Strategies with Thermal Unit Commitment by Introducing Pumped Storage Hydroelectricity & Renewable Energy," *International Conference on Power Electronics and Drive Systems*, Honolulu, USA, pp. 502-506, December 2017.
[36] X. Xu, M. Bishop, D. G. Oikarinen, and C. Hao, "Application and Modeling of Battery Energy Storage in Power Systems," *CSEE Journal of Power and Energy Systems*, Vol. 2, No. 3, pp. 82-90, September 2016.